5138–5150 *Nucleic Acids Research, 2009, Vol. 37, No. 15* *Published online 24 June 2009*
doi:10.1093/nar/gkp541

Comparative analysis of activator-Eσ^{54} complexes formed with nucleotide-metal fluoride analogues

Patricia C. Burrows[1], Nicolas Joly[1], B. Tracy Nixon[2] and Martin Buck[1,*]

[1]Department of Life Sciences, Division of Biology, Faculty of Natural Sciences, Sir Alexander Fleming Building, Imperial College London, London, SW7 2AZ, UK and [2]Department of Biochemistry and Molecular Biology, 406 Frear South Building, Pennsylvania State University, University Park, PA 16802, USA

Received May 6, 2009; Revised June 8, 2009; Accepted June 9, 2009

ABSTRACT

Bacterial RNA polymerase (RNAP) containing the major variant σ^{54} factor forms open promoter complexes in a reaction in which specialized activator proteins hydrolyse ATP. Here we probe binding interactions between σ^{54}-RNAP (Eσ^{54}) and the ATPases associated with various cellular activities (AAA+) domain of the *Escherichia coli* activator protein, PspF, using nucleotide-metal fluoride (BeF and AlF) analogues representing ground and transition states of ATP, which allow complexes (that are otherwise too transient with ATP) to be captured. We show that the organization and functionality of the ADP–BeF- and ADP–AlF-dependent complexes greatly overlap. Our data support an activation pathway in which the initial ATP-dependent binding of the activator to the Eσ^{54} closed complex results in the re-organization of Eσ^{54} with respect to the transcription start-site. However, the nucleotide-dependent binding interactions between the activator and the Eσ^{54} closed complex are in themselves insufficient for forming open promoter complexes when linear double-stranded DNA is present in the initial closed complex.

INTRODUCTION

Bacteria utilize a number of elaborate signalling pathways to ensure that genes are only expressed when required. At the heart of these pathways lie transcription factors which modulate the activity of RNA polymerase (RNAP), the central enzyme in gene expression (1). Bacterial RNAP is a multi-subunit enzyme, comprised of a catalytic core ($\alpha_2\beta\beta'\omega$; E) and a dissociable sigma (σ) subunit which belongs to one of two classes: σ^{70} or σ^{54}. Regulation of transcription can occur on two levels: (i) controlling RNAP promoter binding, as is often the case for the major σ^{70} class (Eσ^{70}) (2,3) or (ii) controlling the DNA melting step, as is the case for the major variant σ^{54} class (Eσ^{54}) (4,5). For Eσ^{54}, DNA melting requires the action of a specialized activator ATPase (also termed bacterial enhancer binding protein, bEBP) belonging to the extended ATPases associated with various cellular activities (AAA+) protein family (6–9). Transcription initiation from σ^{54}-dependent promoters is reminiscent of eukaryotic RNAP II, in that ATP hydrolysis-derived energy, in this case from TFIIH (transcription factor IIH), is a pre-requisite (10,11). Typically bEBPs bind approximately 150 base pairs upstream of the transcription start-site and function to remodel the transcriptionally silent closed complex to the transcriptionally proficient open complex, in which the template DNA strand is found loaded within the RNAP catalytic cleft (12,13).

Much of our understanding about bEBPs originates from the well-studied examples NtrC, NtrC1, NifA, PspF, ZraR, XylR and DctD (8,14–17). Typically bEBPs are composed of three domains: an N-terminal regulatory domain, a central catalytic AAA+ domain and a C-terminal DNA-binding domain (9). The AAA+ domain is often sufficient to activate transcription both *in vivo* and *in vitro* (18). bEBPs contain highly conserved Walker A and B motifs (required for ATP binding and hydrolysis) and a SRH (second region of homology) sequence common to all AAA+ proteins. They also contain two important loop insertions (termed the L1 and L2 loops) within the AAA+ domain (19). The L1 and L2 loops are thought to undergo a series of movements in response to the binding and hydrolysis of ATP. The L1 loop (located within Helix 3) contains a highly conserved GAFTGA motif at its tip, which has been demonstrated to directly interact with Region I of σ^{54} (18). The L2 loop (located at the C-terminus of Helix 4) has been proposed to contact and co-ordinate the movements of the L1 loop (20). Since isomerization of the Eσ^{54} closed complex to the open complex involves a series of intermediate states it seems likely that a number of different binding interactions between the bEBP (mediated via the L1 loop) and Eσ^{54} occur during the ATP hydrolysis cycle.

*To whom correspondence should be addressed. Tel: +44 2075945442; Fax: +44 2075945419; Email: m.buck@imperial.ac.uk

The extent to which binding interactions between bEBPs and $E\sigma^{54}$ re-organize the closed complex and the dependence of these re-organization events upon specific nucleotide-bound states of the bEBPs have been studied at the structural, but not at a functional level (21,22). At present, our understanding includes consideration of several structural studies of the catalytic AAA+ domain of a number of bEBPs, sometimes in association with nucleotide-metal fluoride analogues (23,24) resulting in the formation of stable higher-order oligomers, often hexamers (16,25). These nucleotide-metal fluoride analogues are reported to represent ground state [ATP binding: ADP–BeF (26) and AMP–AlF (27)] and transition state [at the point of ATP hydrolysis: ADP–AlF; (28,29)] ATP analogues. Importantly, stable complexes believed to reflect putative transcription initiation intermediates have been captured between $E\sigma^{54}$ and the AAA+ domain of PspF (residues 1–275; termed $PspF_{1–275}$) using AMP–AlF and ADP–AlF (27,28). Recently, the cryo-EM reconstruction of an $E\sigma^{54}$–$PspF_{1275}$ complex in the presence of ADP–AlF analogue (but in the absence of promoter DNA) was resolved [Figure 1 and (30)]. Interestingly, this $E\sigma^{54}$–$PspF_{1-275}$ structure reveals that upon bEBP binding, a physical block (corresponding to σ^{54} Region I), which would otherwise prevent DNA entry into the RNAP catalytic cleft, is reorganized. This structural study also indicated that $PspF_{1–275}$ (and by inference any bEBP) may further be required to align the promoter DNA for entry into the RNAP catalytic cleft.

Here we comprehensively address the functionalities of $E\sigma^{54}$ promoter complexes formed in the presence of $PspF_{1–275}$ in combination with the established ground state analogue ADP–BeF and the other metal fluoride analogues, ADP–AlF and AMP–AlF. We now provide evidence that the ground and transition state ATP analogues cause some apparently common changes in the σ^{54}–DNA and $PspF_{1-275}$–DNA interactions. Using variants of $PspF_{1–275}$ we identified residues important for formation of the ADP–BeF complex that differ from the residues implicated in formation of the AMP–AlF or ADP–AlF trapped complexes. Specifically residue N64, which forms part of a conformational signalling pathway in PspF (31), appears to be critical for formation of one ground state analogue, ADP–BeF-dependent complex, but not the putative ground state analogue, AMP–AlF-dependent complex. Using photo-cross-linking (to measure the protein–DNA relationship changes) and abortive transcription assays (to measure the enzymatic transcriptional output of the $E\sigma^{54}$ complexes) we demonstrate that ground and transition state ATP analogues support binding interactions between $PspF_{1–275}$ and the $E\sigma^{54}$ promoter DNA complex that are insufficient to produce transcriptionally active complexes on duplex promoter DNA.

MATERIALS AND METHODS

Proteins and DNA probes

Escherichia coli core RNAP was purchased from Epicentre technology (Cambio). *Klebsiella pneumoniae* σ^{54} and *E. coli* $PspF_{1–275}$ wild-type or variants were purified as described (31,32). The *Sinorhizobium meliloti nifH* phosphorothioated (Operon) DNA probes were derivatized with *p*-azidophenacyl bromide at the −12/−11, −8/−7 and −1/+1 position as described (33,34). The (modified) promoter strands were ^{32}P-labelled and annealed to the complementary strand as described (35). The promoter DNA probes (Operon) used in the native gel shift mobility assay were ^{32}P-labelled and annealed to the complementary strand exactly as described (36). For ^{32}P-end labelling, a heart muscle kinase (HMK)-tagged σ^{54} variant was formed (pNJ37), purified and labelled as described (37).

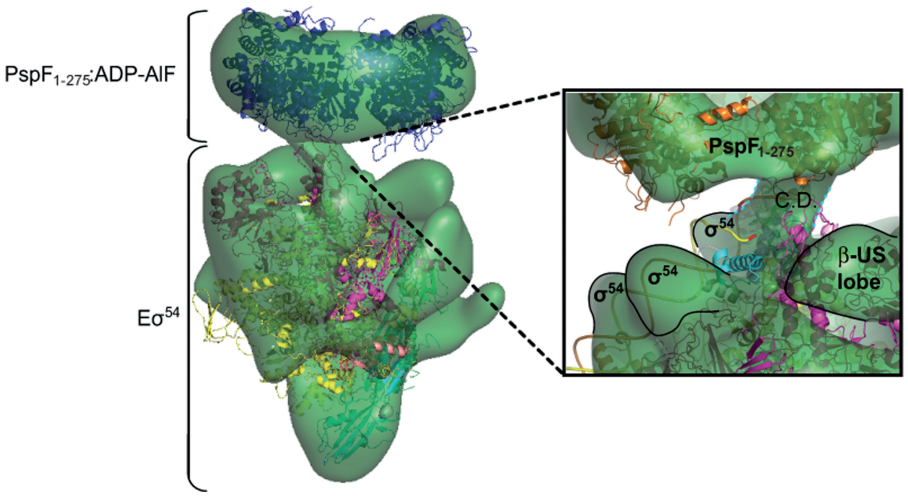

Figure 1. The cryo-electron microscopy structure of the $E\sigma^{54}$–$PspF_{1–275}$:ADP–AlF co-complex (30). The crystal structures of the *Thermus thermophilus* core RNAP and the *Escherichia coli* $PspF_{1–275}$ hexamer have been fitted within the reconstruction and the density attributable to σ^{54} assigned. Enlarged is the region of the reconstruction highlighting the connecting (between PspF and σ^{54}) density (labelled C.D. in the figure), which is proposed to contain the σ^{54}-interacting L1 loop(s) of PspF and as yet unidentified residues of Region I of σ^{54}.

Nucleotide-metal fluoride trapping assays

Nucelotide–metal fluoride trapping experiments were performed in STA buffer (25 mM Tris–acetate, pH 8.0, 8 mM Mg–acetate, 10 mM KCl and 3.5% w/v PEG 6000) in a 10 µl reaction volume containing either 200 nM $E\sigma^{54}$–^{32}P (reconstituted using a 1:4 ratio of $E:\sigma^{54}$) or 1 µM σ^{54}–^{32}P. Trapped complexes were formed in the presence of 5 µM $PspF_{1–275}$ (wild-type or variants), 5 mM NaF and either 1 mM ADP (for ADP–BeF and ADP–AlF reactions) or 1 mM AMP (for AMP–AlF reactions). The 'trapping' reaction was initiated by adding 0.2 mM $BeCl_2$ (for ADP–BeF reactions) or 0.2 mM $AlCl_3$ (for ADP–AlF and AMP–AlF reactions) and incubated for 10 min at 37°C. The samples were analysed by Native-PAGE (4.5%) run at 100 V for 55 min. The gels were dried and protein–DNA complexes visualized and quantified using a FLA-5000 PhosphorImager. These experiments were minimally performed in triplicate.

Native gel mobility shift assays

Native gel mobility assays were conducted in STA buffer in a total reaction volume of 10 µl and contained either 100 nM $E\sigma^{54}$ (reconstituted using a 1:4 ratio of $E:\sigma^{54}$) or 1 µM σ^{54}, which was incubated with 20 nM ^{32}P-labelled probe for 5 min at 37°C. Where indicated 5 µM $PspF_{1–275}$ and the ADP–BeF, ADP–AlF and AMP–AlF trapping reagents were added to the reaction (as described above) and incubated for 5 min at 37°C. Trapped complexes were formed *in situ* by addition of 0.2 mM $BeCl_2$ (for ADP–BeF reactions) or 0.2 mM $AlCl_3$ (for ADP–AlF and AMP–AlF reactions) to the appropriate reaction mix and the sample incubated at 37°C for a further 10 min. The samples were analysed by Native-PAGE (4.5%) run at 100 V for 55 min. The gels were dried and protein–DNA complexes visualized and quantified using a FLA-5000 PhosphorImager. These experiments were minimally performed in triplicate.

Abortive transcription initiation assays

Abortive transcription initiation assays were performed in STA buffer in a 10 µl reaction volume containing 100 nM $E\sigma^{54}$ (reconstituted using a 1:4 ratio of $E:\sigma^{54}$), 20 nM *S. meliloti nifH* promoter probe and either 4 mM dATP or 5 µM $PspF_{1–275}$ and the ADP–BeF, ADP–AlF or AMP–AlF trapping reagents (as indicated above). Open complex formation was initiated by the addition of 5 µM $PspF_{1–275}$ (to the reactions containing dATP) and incubated for 5 min at 37°C. Trapped complexes were formed *in situ* as described above. To test the effect of the trapping reagents on the catalytic activity of $E\sigma^{54}$, we pre-formed open complexes (as described above), and then added the trapping reagents (5 mM NaF, either 1 mM ADP or 1 mM AMP and either 0.2 mM $BeCl_2$ or 0.2 mM $AlCl_3$) to the open complexes and incubated the reaction mix for a further 10 min at 37°C. The synthesis of an abortive transcript (UpGGG) was initiated by adding a mix containing 100 µg/ml heparin, 0.5 mM UpG and 4 µCi [α-^{32}P]GTP and the reaction mix incubated at 37°C for 20 min. The reaction was quenched by addition of loading buffer and analysed on a 20% denaturing gel. Transcripts were visualized and quantified using a Fuji FLA-5000 PhosphorImager. These experiments were minimally performed in triplicate.

Photo-cross-linking assays

Photo-cross-linking reactions were conducted at 37°C in STA buffer in a total reaction volume of 10 µl as previously described (33,38). Briefly, where indicated 20 nM modified ^{32}P-labelled promoter DNA probe, 1 µM σ^{54} or 200 nM $E\sigma^{54}$ holoenzyme (reconstituted using a 1:2 ratio of $E:\sigma^{54}$) and either 4 mM dATP or 5 µM $PspF_{1–275}$ and the trapping reagents (as described above) was incubated for 5 min at 37°C. $PspF_{1–275}$ (5 µM) was then added to the dATP reactions to form open complexes and trapped complexes were formed *in situ* by addition of either $BeCl_2$ or $AlCl_3$ as described above. To eliminate any free core RNAP (in the $E\sigma^{54}$ reactions) from binding the promoter probe, all reactions contained 100 ng/µl salmon sperm DNA. Reactions were UV irradiated at 365 nm for 10 s (in experiments shown in Figure 4) or 30 s (in experiments shown in Figure 5) using a UV-Stratalinker 1800 (Stratagene). A 2 µl sample of the cross-linking reaction was analysed by Native-PAGE (4.5%), run at 100V for 55 min. The remainder of the cross-linking reaction was diluted by addition of 5 µl 10 M Urea and 5 µl 2× SDS loading buffer (Sigma). The samples were heated at 95°C for 3 min and 10 µl loaded onto a 7.5% SDS–PAGE gel run at 200V for 50 min. The gels were dried and cross-linked protein–DNA complexes visualized and quantified using a Fuji FLA-5000 PhosphorImager. The cross-linked proteins were identified using antibodies against either σ^{54}, β/β' or His-tag (for PspF detection) as described (35). These experiments were minimally performed in triplicate.

RESULTS

$PspF_{1–275}$:ADP–BeF supports trapped complex formation with σ^{54}

In combination with the ATP hydrolysis transition state analogue, ADP–AlF, $PspF_{1–275}$ can form stable complexes with $E\sigma^{54}$ and/or σ^{54}, which can be detected in Native-PAGE analysis as 'trapped' complexes that migrate slower than $E\sigma^{54}$ or σ^{54} and contain a hexamer of $PspF_{1–275}$ (39). More recently, ADP was substituted by AMP and the AMP–AlF analogue produced supported stable trapped complex formation (between $PspF_{1–275}$ and either $E\sigma^{54}$ or σ^{54}) (27). The $PspF_{1–275}$:AMP–AlF co-crystal structure suggests that AMP–AlF more closely resembled ATP in its ground state, consistent with the proposal that a binding interaction between $PspF_{1–275}$ and $E\sigma^{54}$ (or σ^{54}) is supported by ATP binding (25,32).

In order to further investigate the actions of ATP ground state analogues upon interactions between $PspF_{1–275}$ and $E\sigma^{54}$ (or σ^{54}), we used the non-hydrolysable ATP analogue ADP–BeF [previously shown to promote stable complex formation between the AAA+ domain of NtrC ($NtrC^C$) (25,26)]. As shown in Figure 2A under saturating conditions incubation of σ^{54} (and $E\sigma^{54}$;

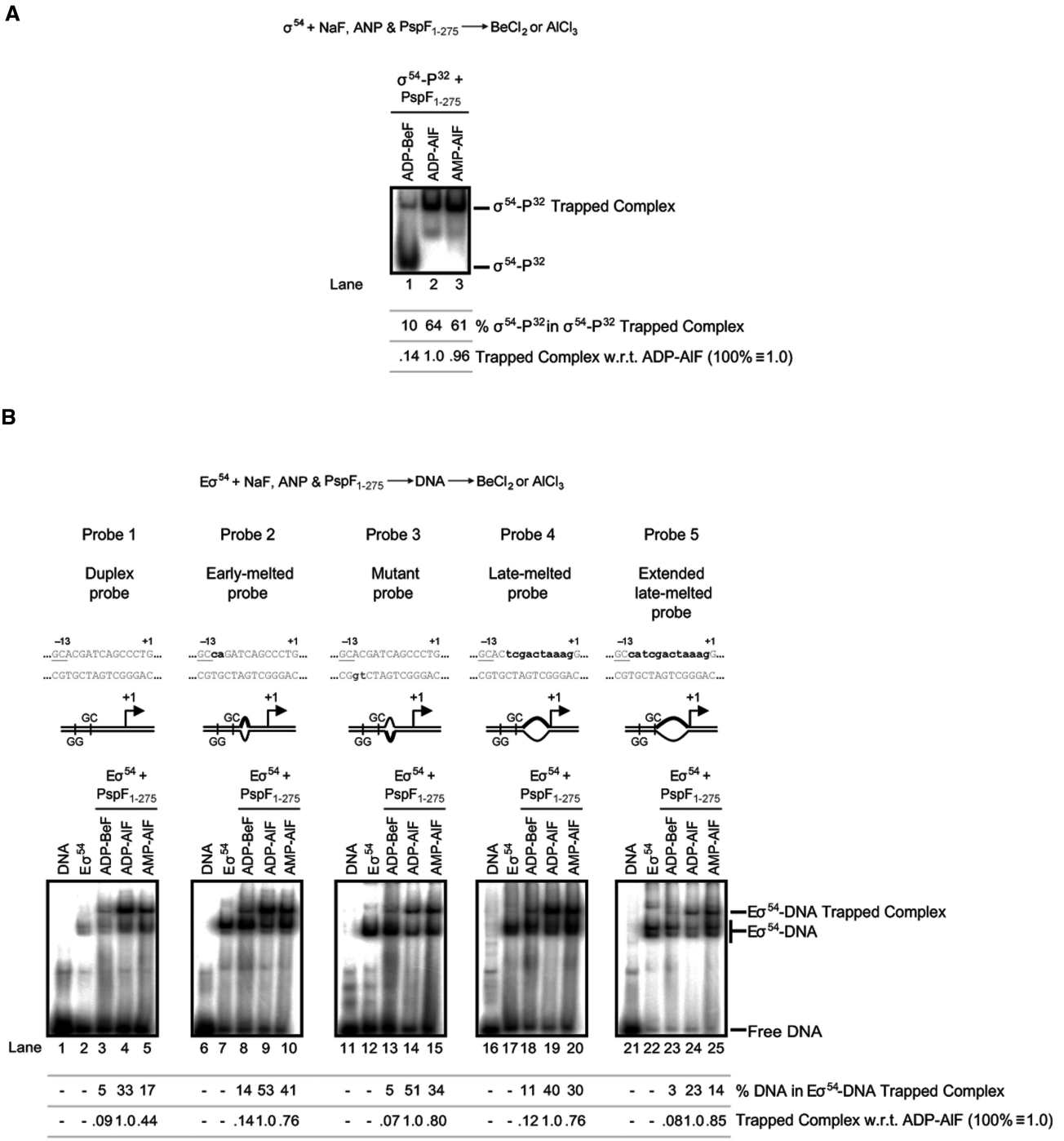

Figure 2. $PspF_{1–275}$:ADP–BeF supports stable trapped complex formation. (**A**) A Native-PAGE gel demonstrating that ^{32}P-labelled σ^{54} (σ^{54}–^{32}P) (and Eσ^{54}–^{32}P; data not shown) can interact with $PspF_{1–275}$ in the presence of the different nucleotide-metal fluoride analogues ADP–BeF (ATP ground state), ADP–AlF (ATP transition state) and AMP–AlF (ATP ground state), to form stable trapped complexes that migrate similarly to one another. A reaction schematic illustrating how trapped complexes were formed is shown above the gel. The migration positions of the σ^{54} trapped complex (σ^{54}–^{32}P trapped complex) and free σ^{54} (σ^{54}–^{32}P) are as indicated. The percentage of ^{32}P-labelled σ^{54} in the trapped complexes is indicated. For comparative purposes we have also expressed the relative intensities of each of the trapped complexes as a percentage of the intensity of the ADP-AlF complex. (**B**) Native gels demonstrating Eσ^{54} trapped complex formation in the presence of promoter DNA probes (labelled probes 1–5) that represent different DNA conformations formed *en route* from the closed to open complex. Probe 1: the duplex probe, is fully double-stranded; probe 2: the early-melted probe, is mismatched at positions −12 and −11 on the non-template strand (mimicking the conformation of DNA in the closed complex); probe 3: the mutant probe, mismatched as in probe 2, but the altered sequence is on the template strand; probe 4: the late-melted probe, contains a non-complementary sequence between positions −10 to −1 (mimics the conformation of DNA in the open complex) and probe 5: the extended late-melted probe, contains a non-complementary sequence between positions −12 to −1. The mismatched sequence is indicated in bold typeface (below the probe schematic). A reaction schematic illustrating how trapped complexes were formed is shown above the gel. The migration positions of the Eσ^{54} DNA trapped (Eσ^{54}–DNA trapped complex) and closed (Eσ^{54}–DNA) complexes and free DNA (Free DNA) are as indicated. Percentage DNA bound in each of the Eσ^{54}–DNA trapped complexes is indicated. For comparative purposes we have also expressed the relative intensities of each of the trapped complexes as a percentage of the intensity of the ADP–AlF complex. In (A and B) the reactions were minimally performed in triplicate and the results obtained followed the same global pattern and were maximally within a ±10% error range.

data not shown) and $PspF_{1–275}$ in combination with the ADP–BeF trapping reagents results in formation of a stable σ^{54}–$PspF_{1–275}$:ADP–BeF (Figure 2A, lane 1) complex which migrates with the same mobility as either the ADP–AlF- (Figure 2A, lane 2) or AMP–AlF-dependent (Figure 2A, lane 3) complexes, suggesting that all of these trapped complexes have a similar composition. Omitting NaF, ADP or $BeCl_2$ (data not shown) demonstrated that formation of the ADP–BeF trapped complex is dependent on formation of the ADP-BeF analogue and not supported by ADP, AlF or BeF alone. Native-PAGE analysis illustrates the stabilities of the trapped complexes are different. The ADP–AlF complex appears the most stable (scored as 100%), the AMP–AlF complex is comparatively as stable (96% of the intensity of the ADP–AlF complex), whereas the ADP–BeF complex seems considerable less stable (only 14% of the intensity of the ADP–AlF complex). These findings are consistent with previous data demonstrating the stabilities of ground state analogue and transition state analogue dependent complexes are not identical (with the ground state being least stable), and taken to suggest that these complexes are distinct from one another (25,40).

Previously it has been shown that His-$PspF_{1–275}$ can form self-associated complexes, independent of σ^{54} in the presence of the ADP–AlF analogue (27,28). We reasoned that given the tendency of His-$PspF_{1–275}$ to form nucleotide-dependent higher-order oligomers, the presence of the His-tag may favour formation of the ADP–BeF complex (without the requirement for σ^{54}). However, we failed to detect any His-$PspF_{1–275}$:ADP–BeF-dependent complexes in the absence of σ^{54} or $E\sigma^{54}$ (data not shown), suggesting that σ^{54} contributes to the stability of the ADP–BeF-dependent complex seen with $PspF_{1–275}$. These data also indicate that the interaction BeF makes with $PspF_{1–275}$ in the absence of σ^{54} is different to that of AlF.

DNA binding is not affected by $PspF_{1–275}$:ADP–BeF

Using a variety of *Sinorhizobium meliloti nifH* promoter DNA probes (Figure 2B, top labelled probes 1–5) we investigated the role of DNA conformation in formation of the DNA trapped complexes (Figure 2B). The promoter DNA probes used here mimic different DNA conformations detected during open complex formation (see Figure 2 legend). We measured by Native-PAGE analysis trapped complex formation between $PspF_{1–275}$ and $E\sigma^{54}$ (Figure 2B) or σ^{54} (data not shown) in the presence of ADP–BeF, ADP–AlF and AMP–AlF.

No obvious probe-specific difference in the DNA-binding properties distinguished any of the trapped complexes (Figure 2B). Promoter DNA also appeared to have no stimulatory effect on formation of the ADP–BeF complex (as judged by Native-PAGE), since no significant increase in the amount of trapped complex was detected in the presence of DNA. However, we can not exclude the possibility that promoter DNA may stabilize ADP–BeF complexes, but not to the extent to survive Native-PAGE analysis. The decreased stability (in terms of Native-PAGE analysis) of the ADP–BeF complex (between 7% and 14% of the intensity of the ADP–AlF complex), compared to either the ADP–AlF or AMP–AlF (which also exhibits reduced Native-PAGE stability of between 44% and 85% of the intensity of the ADP–AlF complex) complexes, may represent an altered arrangement or stabilization of the L1 and L2 loops (within the $PspF_{1–275}$:ADP–BeF complex) with respect to the activator interacting surfaces on σ^{54}, independent of the σ^{54}–DNA interactions (20).

The trapped complexes are transcriptionally inactive

Since the trapped complexes are believed to represent putative intermediates *en route* to the open complex (35), we next considered whether any of these complexes were transcriptionally active. Using an abortive transcription initiation assay (as a measure of open complex formation and which results in the synthesis of a short RNA product, UpGGG) we analysed $E\sigma^{54}$ complexes formed on the super-coiled (SC) *S. meliloti nifH* promoter or a duplex promoter probe (Probe 1). As shown in Figure 3, only within the open complex (i.e. in the presence of $E\sigma^{54}$, $PspF_{1–275}$ and dATP; Figure 3, lane 5) is the abortive product observed. None of the trapped complexes tested (Figure 3; ADP–BeF, lane 2; ADP–AlF, lane 3 and AMP–AlF, lane 4) supported formation of productive open complexes (and hence abortive products) above the level obtained for $E\sigma^{54}$ in the absence of activation (also termed the closed complex; lane 1). Similar results were obtained with full-length transcription assays using the SC template (data not shown). Control reactions demonstrate that (i) the abortive mix can not be used by $PspF_{1–275}$ to support open complex formation (the no nucleotide (NTP) control; Figure 3, lane 6 conducted since PspF can use GTP to form open complexes and the abortive mix contains αGTP; see 'Materials and Methods' section) and (ii) that $PspF_{1–275}$ in the presence of either ADP (Figure 3, lane 7) or AMP (data not shown) rather than dATP or ATP is unable to promote open complex formation.

Importantly, we also established that the trapping reagents had no inhibitory effect on the enzymatic activity of $E\sigma^{54}$, since no significant reduction in the amount of abortive product formed by $E\sigma^{54}$ in the presence of $PspF_{1–275}$ and dATP was observed upon addition of any of the trapping reagents (to pre-formed open complexes, see 'Materials and Methods' section; data not shown). Since open complex formation reflects the loading of melted template DNA within the catalytic cleft of RNAP, we suggest that the absence of abortive transcripts from the trapped complexes is because the steps required for DNA melting and/or delivery of melted DNA into the RNAP catalytic cleft have not yet occurred (as opposed to the trapping reagents simply inhibiting the RNAP catalytic activity). Consistent with this view, using potassium permanganate footprinting (which measures DNA melting) we failed to detect any increased thymine sensitivity at the −8 position (with respect to the transcription start site +1), which is characteristic of melted DNA within the $E\sigma^{54}$ *nifH* open complex (41), within any of the trapped complexes (data not shown)

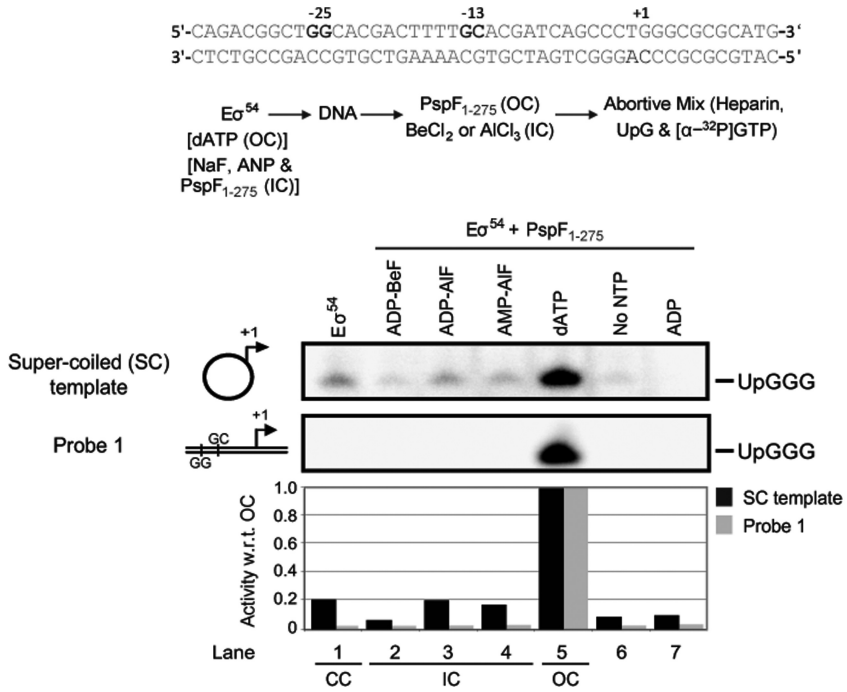

Figure 3. The trapped complexes are transcriptionally inactive. Abortive initiation assays on the (top) super-coiled (SC) and (bottom) duplex *nifH* template (probe 1) demonstrate that only in the presence of $PspF_{1–275}$ and dATP (i.e. the open complex, OC: lane 5) is $E\sigma^{54}$ capable of forming the abortive transcription product UpGGG (see reaction schematic above and 'Materials and Methods' section). The ADP–BeF (lane 2), ADP–AlF (lane 3) and AMP–AlF (lane 4) trapped complexes (i.e. the intermediate complex, IC) are transcriptionally inactive, similar to the profiles of the closed complex (CC) ($E\sigma^{54}$; lane 1), $E\sigma^{54}$ and $PspF_{1–275}$ in the absence of nucleotide (no NTP; lane 6) and $E\sigma^{54}$ and $PspF_{1–275}$ in the presence of either ADP (ADP; lane 7) or AMP (data not shown) but in the absence of the trapping reagents (NaF and either $BeCl_2$ or $AlCl_3$). A reaction schematic illustrating the abortive initiation procedure is shown above the gel. The relative intensities of the abortive products formed on the SC template (black) and probe 1 (grey) are depicted in the bar graph below the gels. The reactions were minimally performed in triplicate and the results obtained followed the same global pattern and were maximally within a ± 10% error range.

(footprints were similar to those obtained with the closed complex). However, it is possible that $PspF_{1–275}$ prevents potassium permanganate from accessing the DNA at this site, or that potassium permanganate may disrupt any trapped complexes containing melted DNA.

Within the trapped complexes the σ^{54}–DNA relationship is altered

Structural studies of the $E\sigma^{54}$–$PspF_{1–275}$:ADP–AlF complex indicate that upon interaction with PspF, Region I of σ^{54} is re-organized (30,42). We reasoned that such re-organization of σ^{54} would also result in an altered σ^{54}-DNA relationship, although the extent of this relationship change in each of the trapped complexes studied here was unknown. To address reorganizations, we used a site-specific photo-cross-linking assay to report changes in σ^{54}–DNA, β/β′-DNA and $PspF_{1–275}$–DNA interactions. The cross-linking reagent *p*-azidophenacyl bromide (APAB; Sigma) was placed between positions −12/−11, −8/−7 and −1/+1 in the context of the duplex probe (probe 1). These sites were chosen based on previous observations revealing that (i) only σ^{54}–DNA interactions are detected within the closed complex (predominantly at position −12/−11) and (ii) upon open complex formation β/β′-DNA interactions are established (33,34).

The SDS-PAGE gels shown in Figure 4 (top panel) illustrate that, consistent with our previous findings, within the closed complex (labelled $E\sigma^{54}$; lanes 1–3) only σ^{54}–DNA interactions are detected at the −12/−11 site (a double band Figure 4, lane 1 arrowed). Within open complexes (the dATP reactions; Figure 4, lanes 13–15) the σ^{54}–DNA cross-links are extended and now detected at the −1/+1 site (Figure 4, lane 15 arrowed), we also observed cross-linked β/β′-DNA (Figure 4, lane 15 arrowed), in line with the loading of template DNA within the RNAP catalytic cleft. Upon formation of the ADP–AlF intermediate complex (Figure 4, lanes 7–9) we observed a more efficient cross-linked σ^{54}–DNA species at the −8/−7 site (single band Figure 4, lane 8 arrowed), but also note a change in the σ^{54}-DNA interactions at the −12/−11 site from a double band (Figure 4, lane 1 arrowed) to a single band (Figure 4, lane 7). The loss of the faster migrating σ^{54}–DNA species may represent the re-organization of σ^{54} (with respect to −12/−11 DNA site) that the structural studies suggested occurred upon interaction with $PspF_{1–275}$:ADP–AlF (30). When we examined the ADP–BeF-dependent (Figure 4, lanes 4–6) and AMP–AlF-dependent (Figure 4, lanes 10–12) trapped complexes, we also observed the same increase in σ^{54}–DNA cross-linking efficiency at the −8/−7 position (Figure 4, lanes 5 and 11) and a change in the −12/−11 σ^{54}–DNA interactions, again from a double band to a

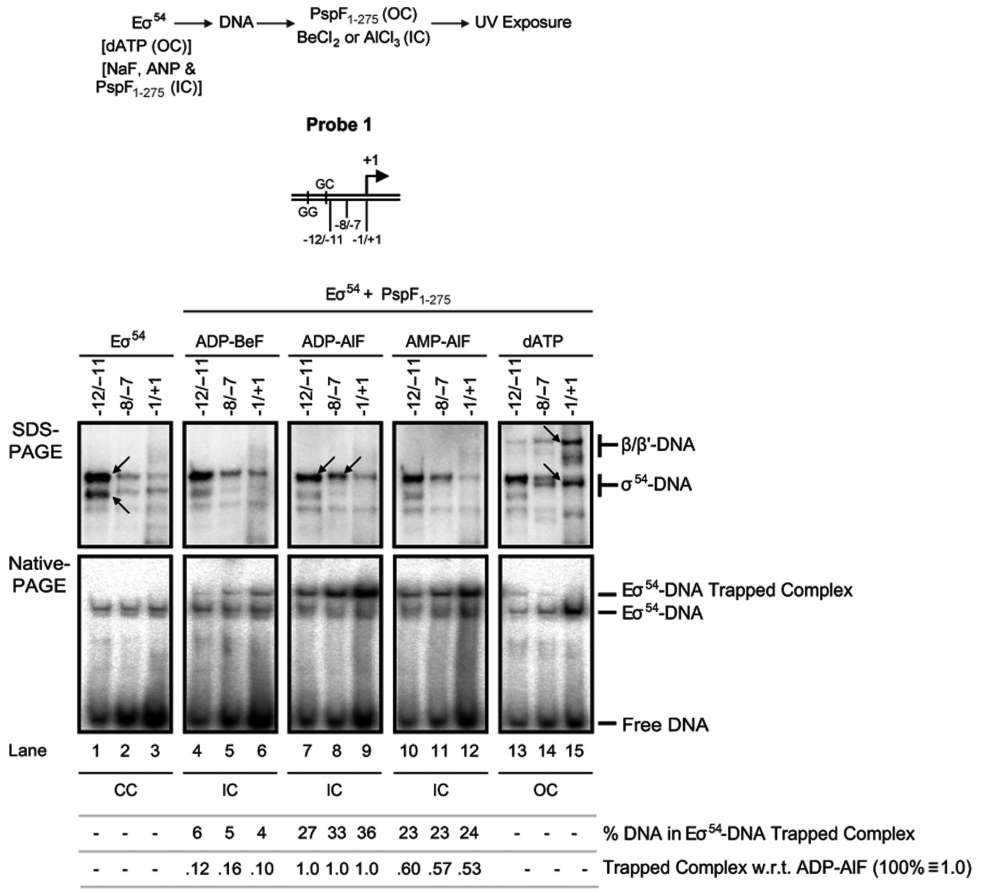

Figure 4. $PspF_{1–275}$:ADP–BeF alters the σ^{54}–DNA interactions. SDS–PAGE (top) and Native-PAGE (bottom) analyses of $E\sigma^{54}$ photo-cross-linking experiments on the duplex promoter probe (probe 1), conjugated with APAB (the photo-cross-linker) at positions −12/−11, −8/−7 and −1/+1. The cross-linking assay demonstrates that all three nucleotide-metal fluoride analogues (ADP–BeF, lanes 4–6; ADP–AlF, lanes 7–9 and AMP–AlF, lanes 10–12) induce the same organizational change in σ^{54}, with respect to promoter position −8/−7 (lanes 5, 8 and 11). However, the organization of σ^{54} is different to that of both the CC ($E\sigma^{54}$; lanes 1–3) and OC (dATP; lanes 13–15). A reaction schematic illustrating the photo-cross-linking procedure is shown above the gel. The migration positions (SDS–PAGE) of the cross-linked β/β′ subunits (β/β′–DNA) and σ^{54} subunit (σ^{54}–DNA) species are as indicated. The migration positions (Native-PAGE) of the $E\sigma^{54}$ DNA trapped ($E\sigma^{54}$–DNA trapped complex) and closed ($E\sigma^{54}$–DNA) complexes and free DNA (Free DNA) are as indicated. Percentage DNA bound in each of the $E\sigma^{54}$–DNA trapped complexes is indicated. For comparative purposes, we have also expressed the relative intensities of each of the trapped complexes as a percentage of the intensity of the ADP–AlF complex. The reactions were minimally performed in triplicate and the results obtained followed the same global pattern and were maximally within a ±10% error range.

single band (Figure 4, lanes 4 and 10). Taken together, these data suggest that the conformational re-organization of σ^{54}, with respect to promoter DNA, induced upon interaction with $PspF_{1–275}$ in each of the trapped complexes is similar. In line with this, copper phenanthroline footprinting [to measure changes in DNA conformation; (41)] demonstrated that the reactivity observed at the −12 site (corresponding to a DNA distortion) within the closed complex, is no longer apparent (data not shown) within the trapped complexes (and is similarly lost in the open complex), suggesting that the $E\sigma^{54}$–DNA organization has changed (within the trapped complexes). However, we can not exclude the possibility that the presence of $PspF_{1–275}$ within the trapped complexes prevents copper phenanthroline accessing the DNA.

Importantly, no DNA cross-linking interactions with the catalytic β/β′ subunits were detected in any of the trapped complexes tested (Figure 4, lanes 4–12), indicating that the template DNA has not yet entered the RNAP catalytic cleft, which is fully consistent with the lack of abortive products observed on the duplex probe (Figure 3). These results again suggest that the trapped complexes, which are distinct from the closed and open complexes (in terms of the relationship between σ^{54} and the β/β′ subunits and the promoter DNA), most likely resemble intermediates formed *en route* to the open complex prior to DNA entering the RNAP catalytic cleft. The cross-linking assay was unable to identify any clear differences at the level of σ^{54}–DNA and β/β′-DNA proximities between the metal fluoride-dependent ''trapped'' complexes (even though the stabilities of these complexes are dissimilar), further suggesting that all three trapped complexes share some common global organization.

The organization of $PspF_{1–275}$ within each of the trapped complexes is similar

We next examined the organization of $PspF_{1-275}$ (with respect to promoter DNA) within the trapped complexes.

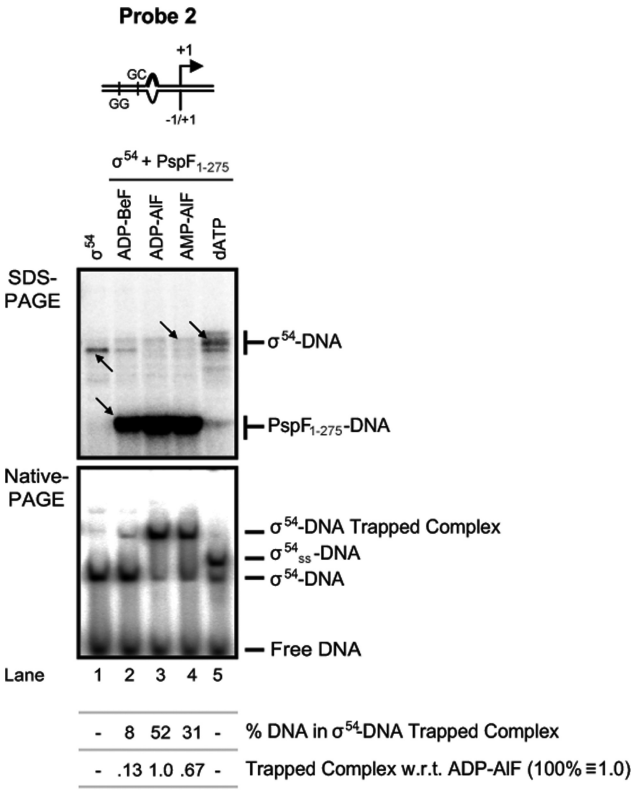

Figure 5. $PspF_{1–275}$ is similarly organized in all the trapped complexes. SDS–PAGE (top) and Native-PAGE (bottom) analyses of σ^{54} photo-cross-linking experiments on the early-melted (probe 2) promoter probe, conjugated at the $-1/+1$ site. In the trapped complexes, $PspF_{1–275}$ is cross-linked to the promoter ($PspF_{1–275}$–DNA). The migration positions (SDS–PAGE) of the cross-linked σ^{54} subunit (σ^{54}–DNA) and $PspF_{1–275}$ ($PspF_{1–275}$–DNA) species are indicated. The migration positions (Native-PAGE) of the σ^{54} DNA trapped (σ^{54}–DNA trapped complex), σ^{54} supershift ($\sigma^{54}{}_{ss}$–DNA) and the binary σ^{54}-probe 2 (σ^{54}–DNA) complexes and free DNA (Free DNA) are as indicated. Percentage DNA bound in each of the σ^{54}–DNA trapped complexes is indicated. For comparative purposes, we have also expressed the relative intensities of each of the trapped complexes as a percentage of the intensity of the ADP–AlF complex. The reactions were minimally performed in triplicate and the results obtained followed the same global pattern and were maximally within a ±10% error range.

Previously we demonstrated that upon increased UV exposure, $PspF_{1–275}$ can be efficiently cross-linked at the $-1/+1$ site in the presence of ADP–AlF (30,33,35). We reasoned that using the extended cross-linking conditions the arrangement of $PspF_{1–275}$ within each of the trapped complexes (ADP–BeF, AMP–AlF and AMP–AlF) could be examined. For clarity we choose to examine the organization of the trapped complexes in the absence of core RNAP on probe 2 (specifically chosen for its σ^{54} binding properties). As shown in Figure 5, upon increased UV exposure we now see a cross-linked σ^{54}–DNA species in the σ^{54} alone reactions (top; Figure 5, lane 1 arrowed). Upon interaction with $PspF_{1–275}$ and dATP, a 'supershift' complex [bottom; Figure 5, lane 5 labelled $\sigma^{54}{}_{ss}$–DNA; (37)] is formed in which the organization of σ^{54} (with respect to the promoter DNA $-1/+1$ site) is altered (double band; Figure 5, lane 5 arrowed compared to a single band; lane 1 arrowed). Interestingly, upon formation of the trapped complexes, the σ^{54}-DNA cross-linked species is now absent (Figure 5, lane 4 arrowed), suggesting that the cross-linking surfaces within σ^{54} are either altered (by $PspF_{1–275}$:ANP–metal fluoride interaction) and/or protected by the $PspF_{1–275}$:ANP–metal fluoride. Within these trapped complexes we also note an additional cross-linked species (Figure 5, lanes 2–4, arrowed lane 2) corresponding to $PspF_{1–275}$–DNA [consistent with our previous findings with ADP–AlF; (30,35)]. Control reactions demonstrated that only in the presence of all the reaction components, which include a form of $PspF_{1–275}$ capable of interacting with σ^{54}, is the cross-linked $PspF_{1–275}$–DNA species detected [data not shown; (33)]. The intensity of the cross-linked $PspF_{1–275}$–DNA species varied amongst the trapped complexes (Figure 5 top, compare lanes 2–4) particularly with respect to the ADP–BeF reactions (Figure 5 top, lane 2). However, we note that the amount of DNA bound within the σ^{54}–DNA–$PspF_{1–275}$:ADP–BeF complex (8%; 13% of the intensity of the ADP–AlF complex) is significantly lower than the amount of DNA bound within either the σ^{54}–DNA–$PspF_{1–275}$:ADP–AlF (52%) or σ^{54}–DNA–$PspF_{1–275}$:AMP–AlF (31%; 67% of the intensity of the ADP–AlF complex) trapped complexes (Figure 5 bottom, compare lanes 2–4), which may account for the difference in the amounts of cross-linked $PspF_{1–275}$–DNA species observed within the ADP–BeF complex versus the ADP–AlF or AMP–AlF complexes.

Interestingly, when we examined the trapped complexes formed on the duplex promoter probe (probe 1) in the presence of core RNAP, we note that the amount of cross-linked $PspF_{1–275}$ DNA species was identical [data not shown; (33)] irrespective of the trapped complex formed. Since the amount of each of the DNA trapped complexes formed varied (similar to the results shown in Figure 2B), we infer that although the ADP–BeF complex is relatively less stable, the organization of $PspF_{1–275}$ with respect to the $-1/+1$ promoter position within each of the trapped complexes (ADP–BeF, ADP–AlF and AMP–AlF) is the same or similar. We also note that PspF in combination with any of the trapping reagents induces a similar conformational re-organization of the σ^{54}–DNA relationship at the $-1/+1$ promoter DNA site as does PspF in the presence of dATP (i.e. within the open complex) does [data not shown; (33)].

Determinants in $PspF_{1–275}$ required for trapped complex formation

Since the global organization of the trapped complexes appeared similar, we next investigated whether formation of the trapped complexes was dependent on similar key residues of PspF (Figure 6A). The $PspF_{1–275}$ variants chosen contained substitutions of residues important for ATP binding and hydrolysis (Walker A; K42 and Walker B; D107) (32,43), a potential R finger residue involved in inter-subunit ATP hydrolysis (R168) (43) and a Walker B interacting residue (N64) (31) (see Figure 1). As a control, we also examined the roles of a surface exposed residue (W56) (44) required for interacting with PspA (which negatively regulates PspF ATPase activity)

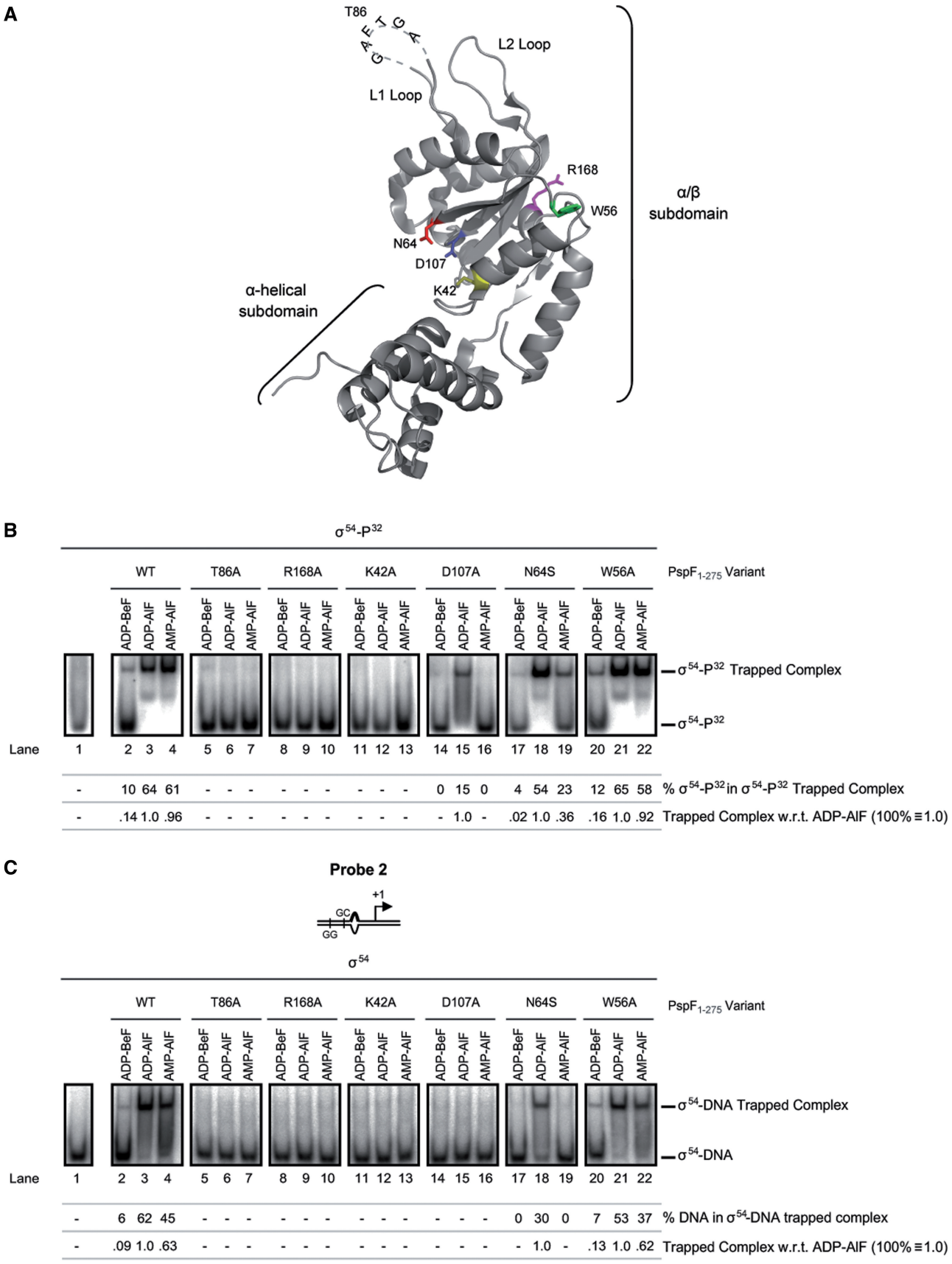

Figure 6. Determinants in $PspF_{1–275}$ required for formation of the trapped complexes. (**A**) The crystal structure of $PspF_{1–275}$ (PDB 2C9C) with the L1 and L2 loop insertions characteristic of bEBPs indicated. We note that the L1 loop is disordered within the crystal structure of $PspF_{1–275}$ and as

that, with the exception of PspA negative regulation, demonstrates wild-type (WT) activities for all other functionalities and the σ^{54}-interacting GAFTGA motif residue T86, which fails to form stable complexes with σ^{54} in the presence of ADP–AlF (45). Initially we examined the role of these residues in formation of stable σ^{54}–$PspF_{1–275}$:ANP–metal fluoride (and $E\sigma^{54}$–$PspF_{1–275}$:ANP–metal fluoride complexes; data not shown) complexes (in a reaction identical to that shown in Figure 2A). As shown in Figure 6B there are two distinct classes of variant: (i) residues essential for forming any of the trapped complexes; T86A (lanes 5–7), R168A (lanes 8–10) and K42A (lanes 11–13) and (ii) residues essential for ADP–BeF- and AMP–AlF-dependent complexes; D107A (Figure 6B, lanes 14–16) and to some extent N64S (Figure 6B, lanes 17–19). The surfaced-exposed W56A (Figure 6B, lanes 20–22) variant behaved identically to WT $PspF_{1–275}$ (Figure 6B, lanes 2–4) in exhibiting no altered trapping activities, supporting the specificity of the differences noted above.

Members of the first class of variants that fail to form any trapped complexes are defective in activities that underlay all nucleotide-dependent binding of PspF to σ^{54} and the closed complex. K42 forms part of the Walker A motif used in nucleotide binding and the K42A variant is an apparent monomer unable to bind nucleotide, R168 has a role in self-association and is believed to interact with the γ-phosphate of ATP during binding and hydrolysis and residue T86 directly interacts with σ^{54}. The inability of these variants to support stable trapped complex formation with any of the nucleotide analogues indicates that when trapped complex formation is observed it has functional and physiological relevance.

Outcomes with the second class of variants speak to the nature of the underlying activities needed to support specific nucleotide-dependent trapping reactions. The D107A variant failed to form any trapped complexes with either ground state analogue (ADP–BeF or AMP–AlF), which may reflect its proposed role in co-ordinating the γ-phosphate of ATP in the initial interaction, prior to ATP hydrolysis occurring. However, we do note that the intensity of the ADP–AlF complex was significantly reduced with this variant and the inability to detect complexes with the ground state analogues may be because they fall below our detection limits. The N64S variant demonstrates an interesting phenotype since the intensity of the ADP–AlF complex is similar to that observed with WT $PspF_{1–275}$, however, the intensities of the AMP–AlF (36% of the intensity of the ADP–AlF complex) and ADP–BeF (2% of the intensity of the ADP–AlF complex) complexes are significantly reduced, suggesting that N64 contributes to the stability of the ground state complexes. However, the contribution N64S makes to each of these complexes is uneven, given that the intensity of the AMP–AlF complex is reduced by ~3-fold, whilst the intensity of the ADP–BeF complex is reduced by ~7-fold, suggesting that the organization of these two ground state analogues are not identical. These results are consistent with the proposed role of N64 in positioning or sensing of the γ-phosphate of ATP and may suggest an involvement in initial ATP binding interactions.

We next assayed σ^{54} trapped complex formation using these PspF variants in the presence of probe 2 (which binds σ^{54} tightly) (in a similar reaction to that of Figure 2B). Interestingly, we note that promoter DNA (Figure 6C) had a significant effect on σ^{54} DNA trapped complex formation in the presence of the D107A (Figure 6C, lanes 14–16) and N64S variants (Figure 6C, lanes 17–19). We note that with D107A, where we previously observed an ADP–AlF-dependent trapped complex (Figure 6B, lane 15) we now fail to detect any (Figure 6C, lane 15), suggesting that either the trapped complex can not accommodate promoter DNA, or the interaction between this PspF variant and σ^{54} is disfavoured when σ^{54} is DNA-bound, presumably because the organization of σ^{54} is altered and the PspF interacting interface may be presented differently. With N64S, formation of stable σ^{54}–DNA trapped complexes with the ground state analogues are abolished, but ADP–AlF-dependent complexes are still detected. In line with this, cross-linking assays with N64S demonstrate that a cross-linked $PspF_{1–275}$N64S–DNA species is only detected within the ADP–AlF-dependent complex (data not shown). The inability of the N64S variant to form trapped complexes which accommodate DNA suggests that the organization of the ground state complexes (particularly AMP–AlF) with this variant are different to that formed with WT $PspF_{1–275}$ (yet the organization of the ADP–AlF complex is similar, if not identical). Importantly, in the presence of DNA the observed difference in the stability (or formation) of trapped complexes formed by the two ground state analogues and N64S is less apparent (given that both analogues fail to be support trapped complex formation). We infer that N64 has an important role in the initial ATP binding events and the subsequent conformational rearrangements in PspF that occur upon nucleotide binding. It would appear that the effects of this variant are

such we have inferred its structure and organization, including the site of the σ^{54} interacting GAFTGA motif (22,39). The positions of residues implicated in ATP binding and hydrolysis (Walker A) K42 (yellow) and (Walker B) D107 (blue), in PspA interaction W56 (and thus negative regulation of the ATPase activity of PspF) (green), a Walker B interacting residue N64 (red), an inter-subunit ATP hydrolysis residue R168 (purple) and σ^{54}-interactions residue T86 (inferred position labelled T86) are as indicated. The role of these determinants in formation of the trapped complexes was assayed in the absence (**B**) (reaction identical to that of Figure 2A) and presence (**C**) (reaction identical to that of Figure 2B) of promoter DNA (we used probe 2 here since σ^{54} binds tightly to this particular probe). For clarity, the data shown here refer to the σ^{54} reactions (in the absence of core RNAP) but are identical to the results obtained in the presence of core RNAP (data not shown). In (B), the migration positions of the σ^{54} trapped complex (σ^{54}–^{32}P trapped complex) and free σ^{54} (σ^{54}–^{32}P) are as indicated. Percentage of ^{32}P-labelled σ^{54} in the σ^{54} trapped complexes is indicated. In (C), the migration positions of the σ^{54} DNA trapped (σ^{54}–DNA trapped complex) and binary σ^{54}–DNA (σ^{54}–DNA) complexes are as indicated. Percentage DNA bound in each of the σ^{54}–DNA trapped complexes is indicated. In (B and C), we have also expressed the relative intensities of each of the trapped complexes as a percentage of the intensity of the ADP–AlF complex. The reactions were minimally performed in triplicate and the results obtained followed the same global pattern and were maximally within a ±10% error range.

more pronounced in the presence of promoter DNA presumably because the organization of σ^{54} (and by inference the PspF-binding interacting interface) is altered upon DNA binding.

DISCUSSION

Transition from the $E\sigma^{54}$ closed complex to a transcription competent open complex is thought to occur via several transient intermediate steps, involving multiple interactions between $E\sigma^{54}$, nucleotide-bound forms of $PspF_{1–275}$ and the promoter DNA. Engagement of the $E\sigma^{54}$ closed complex by PspF (bEBP) requires the appropriate presentation of the surface exposed (σ^{54} interacting) L1 loop, which is determined by the nucleotide-bound state of PspF and also probably depends upon favourable interactions between the L1 and L2 loops (20). To date our understanding of these nucleotide-dependent interactions has been limited to a few structural snapshots and biochemical studies using a limited set of nucleotide-metal fluoride analogues (22,25,27). Using the ATP ground state analogue, ADP–BeF, we have now comprehensively examined the effect of specific nucleotide-bound forms of $PspF_{1–275}$ on σ^{54} ($E\sigma^{54}$) and σ^{54}–DNA ($E\sigma^{54}$–DNA) interactions, and compared these in detail to two other nucleotide-metal fluoride analogues, ADP–AlF (ATP transition state) and AMP–AlF (ATP ground state).

Similar to the nucleotide-metal fluoride analogues ADP–AlF and AMP–AlF, ADP–BeF supports formation of trapped complexes between $PspF_{1–275}$ and either σ^{54} (Figure 2A). However compared to ADP–AlF the stability of ADP–BeF-dependent complexes (judged by Native-PAGE) are severely reduced and not obviously increased by promoter DNA. The differences in the stability of the ground (ADP–BeF) and transition state (ADP–AlF) trapped complexes is not surprising and will be reflected in differences in the precise binding interactions between PspF and the nucleotide analogues. These findings are in line with previous observations where ADP–BeF with $NtrC^{C}$ forms less stable trapped complexes than with ADP–AlF (25). Although different nucleotide analogues are expected to have different off rates differences in the precise interactions PspF makes with the nucleotide-metal fluoride trapped complexes may result in an altered arrangement of the σ^{54}-interacting surfaces to also partly account for differences in the stabilities of the trapped complexes.

The requirement for the functional integrity of residues D107 and N64 for ADP–BeF complex formation with σ^{54} is revealing and consistent given their proposed roles in co-ordinating the γ-phosphate, prior to ATP hydrolysis and in the positioning of the L1 loop (31,32). Mutating either of these residues is predicted to affect the initial interaction of PspF with the γ-phosphate of ATP, but once the β-γ bond is cleaved (potentially represented by the ATP transition state, ADP–AlF) these residues (in particular N64) appears to have a reduced role.

A second condition required for the transition to the open complex may be the requirement for the dissociation of PspF (bEBP) from σ^{54} once a conformational change in σ^{54} has occurred (upon PspF–nucleotide interactions). Changes in the σ^{54} cross-linking pattern caused by $PspF_{1–275}$:ANP–metal fluoride analogues support this view (Figures 4 and 5), in that both the ground and transition state analogues cause some re-organization of the σ^{54}–DNA relationship even though the promoter DNA is not yet melted or delivered into the RNAP catalytic cleft. The cross-linking data also suggests that dissociation of $PspF_{1–275}$ may be required to form transcriptionally proficient open complexes, since within open complexes no cross-linked $PspF_{1–275}$–DNA species is observed (Figure 4 and data not shown). Importantly, the cross-linking data highlights the similarities in all three nucleotide-metal fluoride trapped complexes in terms of the organization of σ^{54}, the catalytic β/β' subunits and $PspF_{1–275}$, regardless of the DNA conformation and the sites of cross-linker incorporation examined. These data support the existence of an activation pathway in which an NTP-bound form of the bEBP binds to the closed complex, resulting in organizational changes in the closed complex with respect to promoter DNA. Apparently these changes persist when the transition state of ATP forms, implying that further changes in organization of $E\sigma^{54}$ apparent in the open complex are subsequently associated with formation of ADP and/or Pi in some of the bEBPs subunits.

Nucleotide metal fluoride analogues are increasingly recognized as sensitive tools to capture structural transitions (46,47) associated with nucleotide binding and hydrolysis that are otherwise too transient to assess. They have been widely employed to study structural and functional intermediates in the wider AAA+ family (46,47) and our results serve to illustrate the subtle yet apparent structural variability that can be achieved using these nucleotide-metal fluoride analogues.

ACKNOWLEDGEMENTS

We thank Dr D. Bose and Prof. X. Zhang for providing the reconstruction of $E\sigma^{54}$–$PspF_{1–275}$:ADP–AlF. We thank Mr C. Engl, Miss E. James and Dr J. Schumacher for valuable comments on the manuscript. We also thank the members of the Buck and Nixon laboratories for helpful discussions and support.

FUNDING

Wellcome Trust [grant number 084599/Z/07/Z to M.B.]; the Biotechnology and Biological Sciences Research Council [grant number BB/G001278/1 to M.B.] and the National Institutes of Health [grant number GM069937 to B.T.N.]. Funding for open access charge: Wellcome Trust [grant number 084599/Z/07/Z].

Conflict of interest statement. None declared.

REFERENCES

1. Ebright,R.H. (2000) RNA polymerase: structural similarities between bacterial RNA polymerase and eukaryotic RNA polymerase II. *J. Mol. Biol.*, **304**, 687–698.

2. Browning,D.F. and Busby,S.J. (2004) The regulation of bacterial transcription initiation. *Nat. Rev. Microbiol.*, **2**, 57–65.
3. Paget,M.S. and Helmann,J.D. (2003) The sigma70 family of sigma factors. *Genome Biol.*, **4**, 203.
4. Buck,M., Gallegos,M.T., Studholme,D.J., Guo,Y. and Gralla,J.D. (2000) The bacterial enhancer-dependent sigma(54) (sigma(N)) transcription factor. *J. Bacteriol.*, **182**, 4129–4136.
5. Merrick,M.J. (1993) In a class of its own—the RNA polymerase sigma factor sigma 54 (sigma N). *Mol. Microbiol.*, **10**, 903–909.
6. Hanson,P.I. and Whiteheart,S.W. (2005) AAA+ proteins: have engine, will work. *Nat. Rev. Mol. Cell. Biol.*, **6**, 519–529.
7. Ogura,T. and Wilkinson,A.J. (2001) AAA+ superfamily ATPases: common structure—diverse function. *Genes Cells*, **6**, 575–597.
8. Rappas,M., Bose,D. and Zhang,X. (2007) Bacterial enhancer-binding proteins: unlocking sigma54-dependent gene transcription. *Curr. Opin. Struct. Biol.*, **17**, 110–116.
9. Studholme,D.J. and Dixon,R. (2003) Domain architectures of sigma54-dependent transcriptional activators. *J. Bacteriol.*, **185**, 1757–1767.
10. Kim,T.K., Ebright,R.H. and Reinberg,D. (2000) Mechanism of ATP-dependent promoter melting by transcription factor IIH. *Science*, **288**, 1418–1422.
11. Lin,Y.C., Choi,W.S. and Gralla,J.D. (2005) TFIIH XPB mutants suggest a unified bacterial-like mechanism for promoter opening but not escape. *Nat. Struct. Mol. Biol.*, **12**, 603–607.
12. Popham,D.L., Szeto,D., Keener,J. and Kustu,S. (1989) Function of a bacterial activator protein that binds to transcriptional enhancers. *Science*, **243**, 629–635.
13. Wedel,A. and Kustu,S. (1995) The bacterial enhancer-binding protein NTRC is a molecular machine: ATP hydrolysis is coupled to transcriptional activation. *Genes Dev.*, **9**, 2042–2052.
14. Fernandez,S., de Lorenzo,V. and Perez-Martin,J. (1995) Activation of the transcriptional regulator XylR of *Pseudomonas putida* by release of repression between functional domains. *Mol. Microbiol.*, **16**, 205–213.
15. Lee,S.Y., De La Torre,A., Yan,D., Kustu,S., Nixon,B.T. and Wemmer,D.E. (2003) Regulation of the transcriptional activator NtrC1: structural studies of the regulatory and AAA+ ATPase domains. *Genes Dev.*, **17**, 2552–2563.
16. Sallai,L. and Tucker,P.A. (2005) Crystal structure of the central and C-terminal domain of the sigma(54)-activator ZraR. *J. Struct. Biol.*, **151**, 160–170.
17. Wang,Y.K., Park,S., Nixon,B.T. and Hoover,T.R. (2003) Nucleotide-dependent conformational changes in the sigma54-dependent activator DctD. *J. Bacteriol.*, **185**, 6215–6219.
18. Bordes,P., Wigneshweraraj,S.R., Schumacher,J., Zhang,X., Chaney,M. and Buck,M. (2003) The ATP hydrolyzing transcription activator phage shock protein F of *Escherichia coli*: identifying a surface that binds sigma 54. *Proc. Natl Acad. Sci. USA*, **100**, 2278–2283.
19. Zhang,X., Chaney,M., Wigneshweraraj,S.R., Schumacher,J., Bordes,P., Cannon,W. and Buck,M. (2002) Mechanochemical ATPases and transcriptional activation. *Mol. Microbiol.*, **45**, 895–903.
20. Burrows,P.C., Schumacher,J., Amartey,S., Ghosh,T., Burgis,T.A., Zhang,X., Nixon,B.T. and Buck,M. (2009) Functional roles of the pre-sensor I insertion sequence in an AAA+ bacterial enhancer binding protein. *Mol. Microbiol.*, in press.
21. De Carlo,S., Chen,B., Hoover,T.R., Kondrashkina,E., Nogales,E. and Nixon,B.T. (2006) The structural basis for regulated assembly and function of the transcriptional activator NtrC. *Genes Dev.*, **20**, 1485–1495.
22. Rappas,M., Schumacher,J., Niwa,H., Buck,M. and Zhang,X. (2006) Structural basis of the nucleotide driven conformational changes in the AAA+ domain of transcription activator PspF. *J. Mol. Biol.*, **357**, 481–492.
23. Chabre,M. (1990) Aluminofluoride and beryllofluoride complexes: a new phosphate analogs in enzymology. *Trends Biochem. Sci.*, **15**, 6–10.
24. Martin,R.B. (1988) Ternary hydroxide complexes in neutral solutions of Al3+ and F. *Biochem. Biophys. Res. Commun.*, **155**, 1194–1200.
25. Chen,B., Doucleff,M., Wemmer,D.E., De Carlo,S., Huang,H.H., Nogales,E., Hoover,T.R., Kondrashkina,E., Guo,L. and Nixon,B.T. (2007) ATP ground- and transition states of bacterial enhancer binding AAA+ ATPases support complex formation with their target protein, sigma54. *Structure*, **15**, 429–440.
26. Yan,D., Cho,H.S., Hastings,C.A., Igo,M.M., Lee,S.Y., Pelton,J.G., Stewart,V., Wemmer,D.E. and Kustu,S. (1999) Beryllofluoride mimics phosphorylation of NtrC and other bacterial response regulators. *Proc. Natl Acad. Sci. USA*, **96**, 14789–14794.
27. Joly,N., Rappas,M., Buck,M. and Zhang,X. (2008) Trapping of a transcription complex using a new nucleotide analogue: AMP aluminium fluoride. *J. Mol. Biol.*, **375**, 1206–1211.
28. Chaney,M., Grande,R., Wigneshweraraj,S.R., Cannon,W., Casaz,P., Gallegos,M.T., Schumacher,J., Jones,S., Elderkin,S., Dago,A.E. *et al.* (2001) Binding of transcriptional activators to sigma 54 in the presence of the transition state analog ADP-aluminum fluoride: insights into activator mechanochemical action. *Genes Dev.*, **15**, 2282–2294.
29. Kleuss,C., Raw,A.S., Lee,E., Sprang,S.R. and Gilman,A.G. (1994) Mechanism of GTP hydrolysis by G-protein alpha subunits. *Proc. Natl Acad. Sci. USA*, **91**, 9828–9831.
30. Bose,D., Pape,T., Burrows,P.C., Rappas,M., Wigneshweraraj,S.R., Buck,M. and Zhang,X. (2008) Organization of an activator-bound RNA polymerase holoenzyme. *Mol. Cell*, **32**, 337–346.
31. Joly,N., Burrows,P.C. and Buck,M. (2008) An intra-molecular route for coupling ATPase activity in AAA+ proteins for transcription activation. *J. Biol. Chem.*, **283**, 13725–13735.
32. Joly,N., Rappas,M., Wigneshweraraj,S.R., Zhang,X. and Buck,M. (2007) Coupling nucleotide hydrolysis to transcription activation performance in a bacterial enhancer binding protein. *Mol. Microbiol.*, **66**, 583–595.
33. Burrows,P.C., Joly,N., Cannon,W.V., Camara,B.P., Rappas,M., Zhang,X., Dawes,K., Nixon,B.T., Wigneshweraraj,S.R. and Buck,M. (2009) Coupling sigma factor conformation to RNA polymerase reorganisation for DNA melting. *J. Mol. Biol.*, **387**, 306–319.
34. Burrows,P.C., Wigneshweraraj,S.R. and Buck,M. (2008) Protein–DNA interactions that govern AAA+ activator-dependent bacterial transcription initiation. *J. Mol. Biol.*, **375**, 43–58.
35. Burrows,P.C., Severinov,K., Buck,M. and Wigneshweraraj,S.R. (2004) Reorganisation of an RNA polymerase–promoter DNA complex for DNA melting. *Embo J.*, **23**, 4253–4263.
36. Wigneshweraraj,S.R., Nechaev,S., Bordes,P., Jones,S., Cannon,W., Severinov,K. and Buck,M. (2003) Enhancer-dependent transcription by bacterial RNA polymerase: the beta subunit downstream lobe is used by sigma 54 during open promoter complex formation. *Methods Enzymol.*, **370**, 646–657.
37. Cannon,W.V., Gallegos,M.T. and Buck,M. (2000) Isomerization of a binary sigma-promoter DNA complex by transcription activators. *Nat. Struct. Biol.*, **7**, 594–601.
38. Burrows,P.C., Wigneshweraraj,S., Bose,D., Joly,N., Schumacher,J., Rappas,M., Pape,T., Stockley,P.G., Zhang,X. and Buck,M. (2008) Visualizing the organization and reorganization of transcription complexes for gene expression. *Biochem. Soc. Trans.*, **36**, 776–779.
39. Rappas,M., Schumacher,J., Beuron,F., Niwa,H., Bordes,P., Wigneshweraraj,S., Keetch,C.A., Robinson,C.V., Buck,M. and Zhang,X. (2005) Structural insights into the activity of enhancer-binding proteins. *Science*, **307**, 1972–1975.
40. Ponomarev,M.A., Timofeev,V.P. and Levitsky,D.I. (1995) The difference between ADP-beryllium fluoride and ADP-aluminium fluoride complexes of the spin-labeled myosin subfragment 1. *FEBS Lett.*, **371**, 261–263.
41. Morris,L., Cannon,W., Claverie-Martin,F., Austin,S. and Buck,M. (1994) DNA distortion and nucleation of local DNA unwinding within sigma-54 (sigma N) holoenzyme closed promoter complexes. *J. Biol. Chem.*, **269**, 11563–11571.
42. Leach,R.N., Gell,C., Wigneshweraraj,S., Buck,M., Smith,A. and Stockley,P.G. (2006) Mapping ATP-dependent activation at a sigma54 promoter. *J. Biol. Chem.*, **281**, 33717–33726.
43. Schumacher,J., Zhang,X., Jones,S., Bordes,P. and Buck,M. (2004) ATP-dependent transcriptional activation by bacterial PspF AAA+ protein. *J. Mol. Biol.*, **338**, 863–875.
44. Elderkin,S., Bordes,P., Jones,S., Rappas,M. and Buck,M. (2005) Molecular determinants for PspA-mediated repression of the AAA transcriptional activator PspF. *J. Bacteriol.*, **187**, 3238–3248.

45. Bordes,P., Wigneshweraraj,S.R., Chaney,M., Dago,A.E., Morett,E. and Buck,M. (2004) Communication between Esigma(54), promoter DNA and the conserved threonine residue in the GAFTGA motif of the PspF sigma-dependent activator during transcription activation. *Mol. Microbiol.*, **54**, 489–506.
46. Costa,A., Pape,T., van Heel,M., Brick,P., Patwardhan,A. and Onesti,S. (2006) Structural basis of the Methanothermobacter thermautotrophicus MCM helicase activity. *Nucleic Acids Res.*, **34**, 5829–5838.
47. DeLaBarre,B. and Brunger,A.T. (2003) Complete structure of p97/valosin-containing protein reveals communication between nucleotide domains. *Nat. Struct. Biol.*, **10**, 856–863.